Journal of Assisted Reproduction and Genetics
https://doi.org/10.1007/s10815-020-01721-w

GENETICS

Patients with severe asthenoteratospermia carrying *SPAG6* or *RSPH3* mutations have a positive pregnancy outcome following intracytoplasmic sperm injection

Huan Wu[1,2,3] · Jiajia Wang[1,2,3] · Huiru Cheng[1,2,3] · Yang Gao[1] · Wangjie Liu[6,7,9] · Zhiguo Zhang[1,4,5] · Huanhuan Jiang[1,4,5] · Weiyu Li[6,7,9] · Fuxi Zhu[1,4,5] · Mingrong Lv[1,4,5] · Chunyu Liu[6,7,8,9] · Qing Tan[10] · Xiaofeng Zhang[8] · Chao Wang[1,4,5] · Xiaoqing Ni[1] · Yujie Chen[1] · Bing Song[1,4,5] · Ping Zhou[1,4,5] · Zhaolian Wei[1,4,5] · Feng Zhang[6,7,9] · Xiaojin He[1,2,3] · Yunxia Cao[1,2,3]

Received: 21 October 2019 / Accepted: 13 February 2020

Abstract

Purpose To investigate the relation between mutations in ciliopathy-related *SPAG6* and *RSPH3* and male infertility with severe asthenoteratospermia characterized by multiple flagellar malformations and reveal the intracytoplasmic sperm injection (ICSI) outcomes of those primary ciliary dyskinesia (PCD) patients.

Methods Whole-exome sequencing was applied to identify the pathogenic genes for the five PCD patients. The ICSI outcomes of those patients were compared with eight *DNAH1*-mutated patients and 215 oligo-asthenospermia (OAT) patients.

Results We identified, for the first time, the compound heterozygous *SPAG6* mutations (c.143_145del: p.48_49del, c.585delA: p.Lys196Serfs*6) in a sporadic PCD patient. Further, a novel homozygous nonsynonymous *RSPH3* mutation (c.C799T: p.Arg267Cys) was identified in another PCD patient with consanguineous parents. The pathogenicity of these mutations in the assembly of sperm flagella was confirmed by flagellar ultrastructure analysis, immunofluorescence, and quantitative real-time PCR. All five patients underwent six ICSI cycles. The fertilization rate, blastocyst development rate, and clinical pregnancy rate were 69.3%, 50.0%, and 66.7%, respectively. Four of the five couples, including the subjects carrying mutations in *SPAG6* or *RSPH3*, got healthy children born after ICSI.

Huan Wu, Jiajia Wang and Huiru Cheng contributed equally to this work.

Electronic supplementary material The online version of this article (https://doi.org/10.1007/s10815-020-01721-w) contains supplementary material, which is available to authorized users.

✉ Xiaojin He
hxj0117@126.com

✉ Yunxia Cao
caoyunxia6@126.com

[1] Reproductive Medicine Center, Department of Obstetrics and Gynecology, The First Affiliated Hospital of Anhui Medical University, No 218 Jixi Road, Hefei 230022, Anhui, China

[2] NHC Key Laboratory of Study on Abnormal Gametes and Reproductive Tract, Anhui Medical University, No 81 Meishan Road, Hefei 230032, Anhui, China

[3] Key Laboratory of Population Health Across Life Cycle, Anhui Medical University, Ministry of Education of the People's Republic of China, No 81 Meishan Road, Hefei 230032, Anhui, China

[4] Anhui Province Key Laboratory of Reproductive Health and Genetics, No 81 Meishan Road, Hefei 230032, Anhui, China

[5] Biopreservation and Artificial Organs, Anhui Provincial Engineering Research Center, Anhui Medical University, No 81 Meishan Road, Hefei 230032, Anhui, China

[6] Shanghai Key Laboratory of Female Reproductive Endocrine Related Diseases, Shanghai 200011, China

[7] Obstetrics and Gynecology Hospital, NHC Key Laboratory of Reproduction Regulation (Shanghai Institute of Planned Parenthood Research), State Key Laboratory of Genetic Engineering at School of Life Sciences, Fudan University, Shanghai 200011, China

[8] Department of Pulmonary and Critical Care Medicine, The Third Affiliated Hospital of Anhui Medical University, Hefei 230061, China

[9] State Key Laboratory of Reproductive Medicine, Center for Global Health, School of Public Health, Nanjing Medical University, Nanjing 211116, China

[10] Anhui Provincial Human Sperm Bank, The First Affiliated Hospital of Anhui Medical University, Hefei 230022, China

Published online: 02 March 2020

Additionally, the ICSI outcomes of the five PCD couples were statistically comparable with those of the eight *DNAH1*-mutated couples and the 215 OAT couples.

Conclusions Mutations in ciliopathy-related *SPAG6* and *RSPH3* cause severe asthenoteratospermia characterized by multiple flagellar malformations, resulting in sterility. ICSI is an optimal management with a positive pregnancy outcome.

Keywords Male infertility · *SPAG6* · *RSPH3* · PCD · Asthenoteratospermia · ICSI

Introduction

Primary ciliary dyskinesia (PCD [MIM: 244400]) comprises a rare and genetically heterogeneous recessive disorder with an incidence of 1:15,000–30,000 [1]. This congenital syndrome is characterized by structural and functional defects of respiratory cilia and spermatozoal flagella that leads to bronchiectasis, chronic sinusitis, recurrent respiratory infections, situs inversus, and male infertility [2, 3]. Several genes, involved in the biogenesis of axoneme, have been reported to be associated with PCD, accounting for approximately 70% of affected individuals [4, 5]. Defects in *SPAG6* (MIM: 605730) and *RSPH3* (MIM: 615876) were demonstrated to be the recurrent genetic causes of PCD in human or knockout mouse models [6, 7]. Both genes, encoding the axonemal radial spokes-stalk protein or central microtubules protein, are abundantly expressed in respiratory and testicular tissues. Nevertheless, the phenotype of PCD-associated male infertility caused by the defects of these two ciliopathy-related genes has been scarcely described.

In our study, five unrelated Chinese male infertile PCD patients with severe asthenoteratospermia were recruited. Four of them were born from consanguineous parents. Whole-exome sequencing (WES) was employed to identify the single-nucleotide variants (SNVs) and small insertions or deletions (indels) that may potentially be responsible for PCD. Additionally, we sought to report the ICSI outcome of the five PCD patients. Mutation screening for the identified pathogenic genes in the patients' partners has to be done before ICSI to avoid the inheritance to their offspring. Further, the ICSI outcomes were compared with eight *DNAH1*-mutated patients with multiple morphological abnormalities of the sperm flagella (MMAF) and a group of 215 oligo-asthenospermia (OAT) patients, respectively.

Herein, we report, for the first time, the compound heterozygous mutations in *SPAG6* in an infertile PCD patient with severe asthenoteratospermia. Meanwhile, one novel homozygous nonsynonymous mutation in *RSPH3* was identified in another infertile PCD patient. We verified the pathogenicity of these novel mutations in the assembly of sperm flagella. Moreover, we show the outcomes of ICSI for those infertile PCD patients,

Table 1 Spermatozoal parameters and morphology of the PCD patients

	P1		P2		P3		P4		P5	
	Sample 1	Sample 2	Sample 1	Sample 2	Sample 1	Sample 2	Sample 1	Sample 2	Sample 1	Sample 2
Semen parameters										
Sperm volume (ml)	2.2	3.1	4.3	3.1	3.3	2.4	1.8	3.7	2.7	2.0
Sperm concentration (10^6/ml)	22.7	19.9	17.3	20.4	30.7	20.1	6.9	18.9	17.7	30.1
Progress motility (%)	0.0	0.0	0.0	0.0	0.0	0.0	0.0	0.0	0.0	0.0
Motility (%)	0.0	0.0	1.6	0.5	0.0	0.5	0.8	1.0	1.5	1.8
Sperm morphology										
Abnormal head (%)	72.5		52.0		39.0		47.5		59.5	
Short flagella (%)	62.0		38.5		58.5		46.5		52.5	
Coiled flagella (%)	28.0		51.5		33.5		43.5		36.0	
Absent flagella (%)	4.5		3.5		4.5		2.0		4.5	
Bent flagella (%)	5.0		1.5		0.5		3.5		1.0	
Irregular caliber (%)	0.5		1.0		0		1.0		2.0	
Normal flagella (%)	0.0		4.0		3.0		3.5		4.0	
Normal spermatozoa (%)	0.0		1.5		1.0		2.0		2.5	

The normal value of the semen parameters were according to WHO (2010) Manual criteria

PCD, primary ciliary dyskinesia

which are comparable with the MMAF and OAT patients.

Material and methods

Patients and controls

Five Chinese PCD patients with severe asthenospermia were recruited when they consulted for primary infertility in the Reproductive Medicine Center at the First Affiliated Hospital of Anhui Medical University, between April 2016 and January 2018. The patients were unrelated and four of them had consanguineous parents (first cousins). All patients suffered from chronic sinusitis and recurrent respiratory tract infections since childhood. Computed tomography (CT) scan confirmed bronchiectasis and excluded situs inversus in them (Fig. S1). Testicular volume, sex hormone levels, and somatic karyotype were normal in all patients and Y chromosome microdeletions were not identified in any of them. The ICSI outcomes of eight *DNAH1*-mutated MMAF patients and 215 OAT patients were retrospectively reviewed. The *DNAH1* mutations identified by WES are presented in Figure S2. Control samples were obtained from fertile anonymous donors with normal spermatogenesis. This research was approved by the ethical committee of The First Affiliated Hospital of Anhui Medical University. All PCD patients and their siblings and parents accepted to participate in this study and signed informed consent.

Sperm analysis

According to the World Health Organization (WHO) criteria, sperm parameters and morphology were evaluated by the computer-aided semen analysis system and H&E staining. Referring to MMAF, the malformations of sperm flagella were sorted into five categories: short, coiled, absent, bent, and irregular caliber flagella. One morphological category was identified depending on the predominant abnormality of the flagellum.

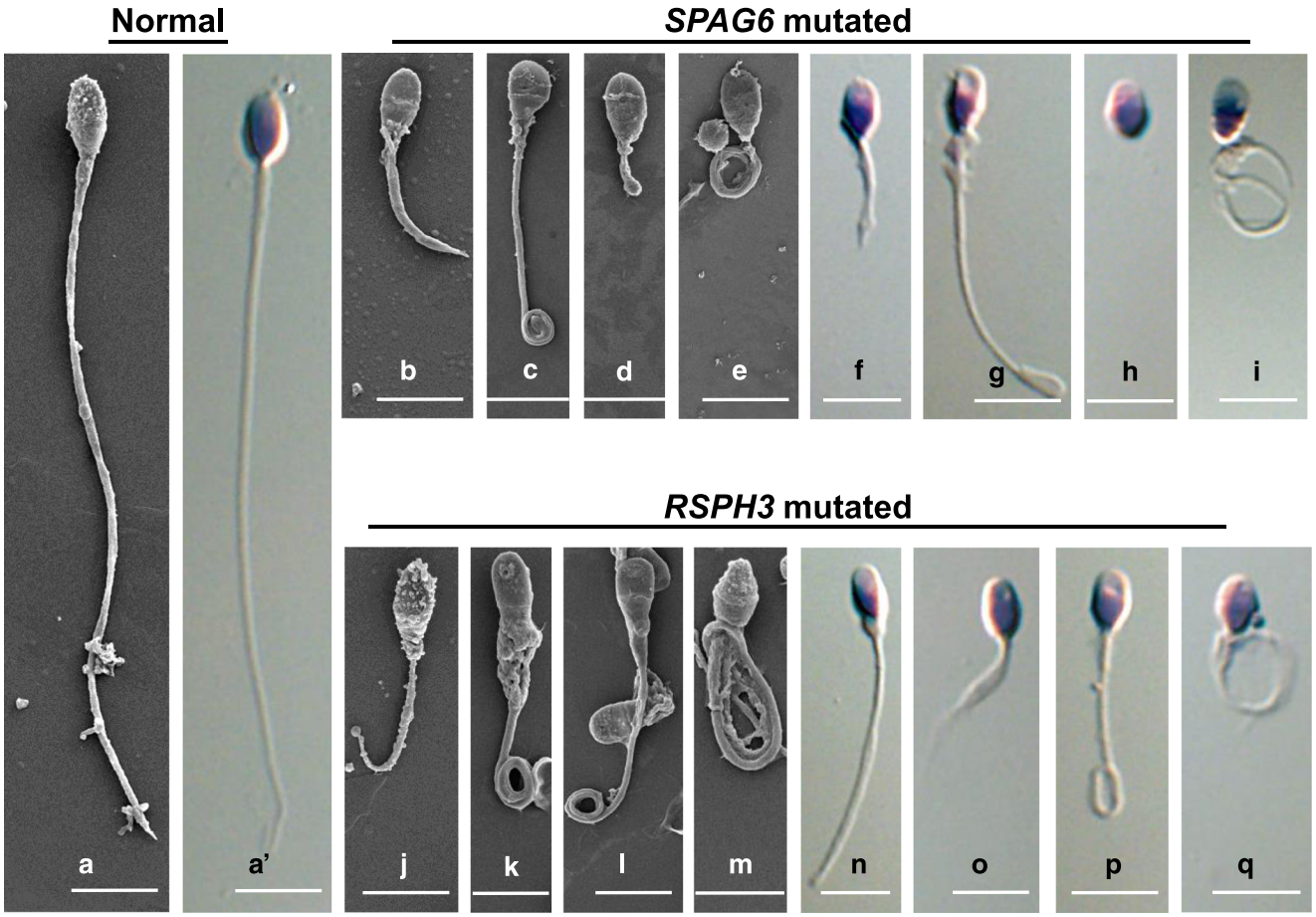

Fig. 1 Morphological defects of the sperm flagella resulting in *SPAG6* and *RSPH3* mutations. (A and A′) Normal morphology of spermatozoa from a healthy control man. (B–E) and (J–M) Scanning electron microscopy images and (F–I) and (N–Q) H&E staining images showed the multiple abnormalities of the sperm flagella from *SPAG6*-mutated proband and *RSPH3*-mutated proband, respectively, including (B, F, J, and O) short, (C, E, I, K, L, M, P, and Q) coiled, (D, H, and L) absent, and (G and N) bent. Scale bars represent 5 μm

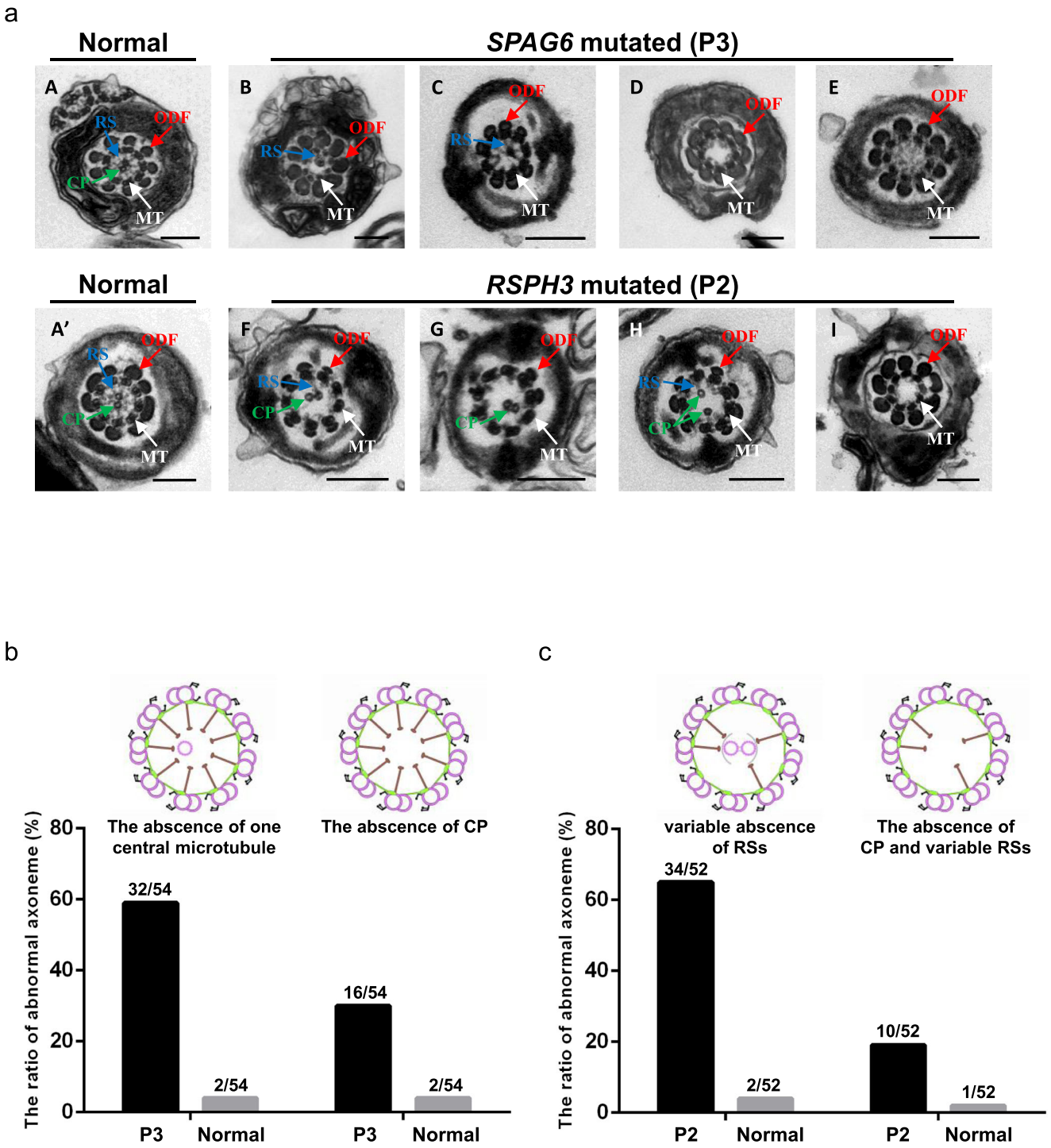

Fig. 2 Transmission electron microscopy of the sperm flagella from the patients with mutations in *SPAG6* and *RSPH3*. (a) Cross-sectional ultrastructure images clearly displayed (A and A′) the normal anoneme with a typical "9 + 2" microtubule structure from a healthy control man. The central pair of microtubules (CP) were surrounded by the nine peripheral doublet microtubules and the microtubules were connected by radial spokes (RSs). (B, C, and b) 59.3% cross-sectional ultrastructures of flagella from *SPAG6*-mutated patient (P3) presented a "9 + 1" microtubule structure lacking one of the CP. (D, E, and b). The other 29.6% cross-sectional ultrastructures from the patient presented a "9 + 0" microtubule structure lacking the CP. The classified ultrastructural defects accounted for 3.7% in the control sample respectively. (F–H and c) 65.4% cross-sectional ultrastructures of flagella from *RSPH3*-mutated patient (P2) presented a "9 + 2" microtubule structure lacking variable RSs. (I and c) The other 19.2% cross-sectional ultrastructures from the patient presented a "9 + 0" microtubule structure lacking the CP and variable RSs. The classified ultrastructural defects accounted for 3.8% and 1.9% in the control sample, respectively. Scale bars of A: 200 nm

Electron microscopy

The prepared sperm cells were immersed in 2% glutaraldehyde, fixed with 1% osmium tetroxide, and embedded in a resin mixture. Then, the cut sections were stained and the ultrastructural defects of sperm flagella were confirmed by scanning and transmission electron microscopy (S/TEM, TECNAI-10, 80 kV, Philips, Holland).

Genetic analysis and Sanger sequencing

WES and bioinformatic analysis were conducted according to our previously described protocols [8]. Sanger sequencing was used to verify the identified mutations and their parental origins. The exons and intron boundaries of *SPAG6* or *RSPH3* in the probands' respective partner were also screened by direct Sanger sequencing. PCR primers are listed in Table S1.

Quantitative real-time PCR experiments

Quantitative real-time PCR (q-PCR) experiments were carried out as described in our previous study [9]. Total RNA was extracted from the purified sperm using TRIzol reagent (Invitrogen, USA). The primers used in q-PCR analyses were listed in Table S2.

Immunofluorescence staining

Protein visualization by immunofluorescence (IF) was carried out as described in our previous study [9]. The primary antibodies used were as follows: rabbit polyclonal anti-SPAG6 antibody 1:100 (Sigma, life science, USA), rabbit polyclonal anti-RSPH3 antibody 1:100 (Proteintech Group, USA), mouse monoclonal anti-tubulin, acetylated antibody 1:500 (Sigma, life science, USA). The secondary antibodies used were as follows: Donkey anti-rabbit IgG H&L 1:500 (Alexa Fluor 488) (ab150073), Donkey anti-mouse IgG H&L 1:500 (Alexa Fluor 594) (ab150108), and Hoechst dye (Thermo Scientific, USA). Slides were observed in a LSM800 confocal microscope (Carl Zeiss, Germany).

Assisted reproductive procedures

Multiple follicular growth was induced by a long protocol of controlled ovarian stimulation between September 2016 and May 2018. The processes were conducted according to our previous description [10]. Sperm samples were processed by discontinuous density gradient centrifugation. Subsequently, metaphase II stage oocytes and motile sperm were selected for ICSI using a micromanipulator system (Olympus, Japan). For samples with total immotile sperm, sperm viability was assessed using the ICSI pipette to test the elasticity of the sperm tail [11]. Eighteen to 19 h later, the fertilized oocytes

Table 2 Genetic study of the patients carrying mutations in *SPAG6* and *RSPH3*

Patient	Gene	cDNA mutation	Protein alteration	Zygosity	Exon	Mutation type	Allele frequency			Deleterious prediction		
							1KGP	ExAC	gnomAD	SIFT	PolyPhen-2	Mutation Taster
P3	*SPAG6*	c.143_145del	p.48_49del	Heterozygous	Exon 3	Non-frameshift deletion	NA	NA	NA	NA	NA	NA
		c.585delA	p.Lys196Serfs*6	Heterozygous	Exon 5	Frameshift deletion	NA	8.25×10^{-6}	4.07×10^{-6}	NA	NA	NA
P2	*RSPH3*	c.C799T	p.Arg267Cys	Homozygous	Exon 4	Nonsynonymous mutations	0.002	0.0002	0.0002	D	D	D

The GenBank accession numbers of *SPAG6* and *RSPH3* are NM_012443 and NM_031924, respectively

1KGP, 1000 Genomes Project; *ExAC*, Exome Aggregation Consortium; *gnomAD*, Genome Aggregation Database; *NA*, not available; *D*, disease causing

a

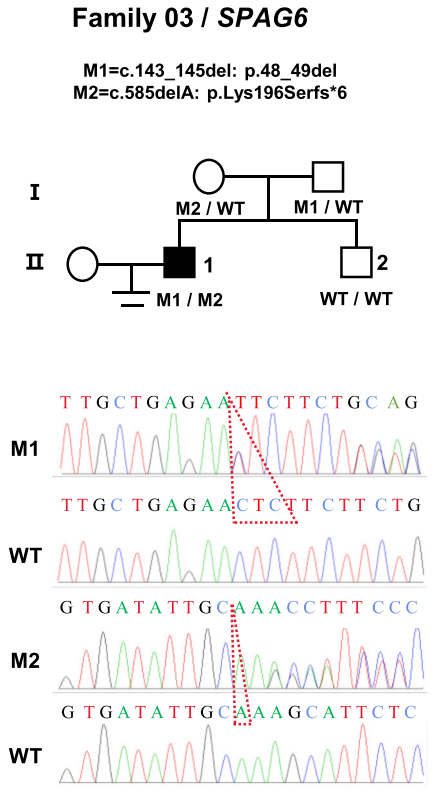

b

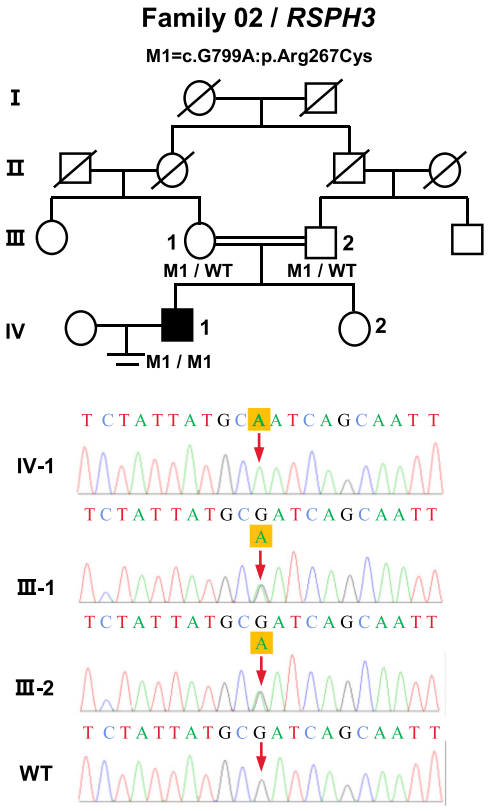

c

SPAG6-hg19: ENST00000576624.8

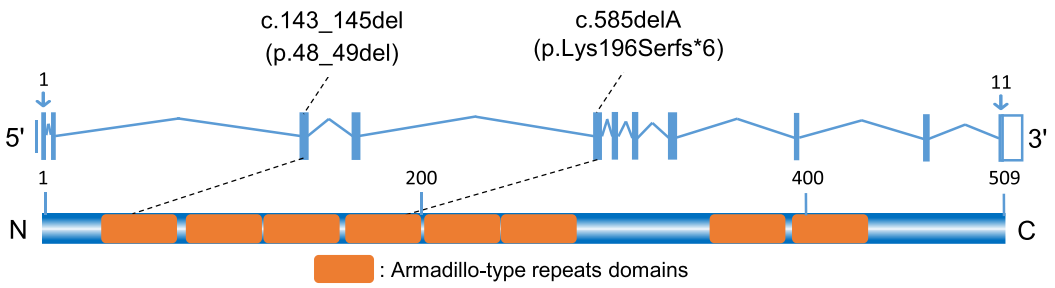

d

RSPH3-hg19: ENST00000252655.1

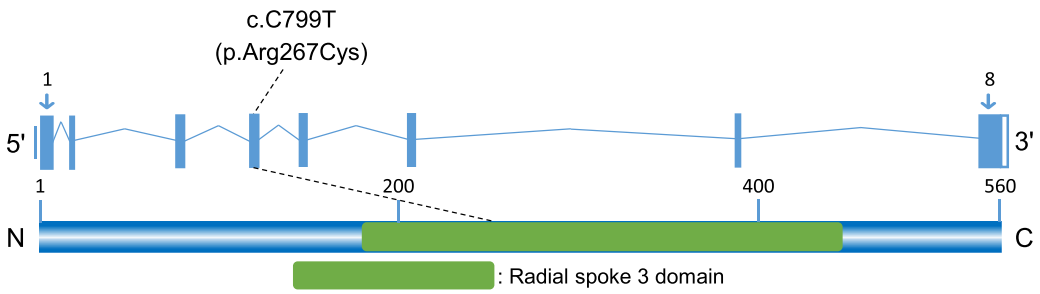

◀ **Fig. 3** Mutations in *SPAG6* and *RSPH3* were identified in Chinese men with PCD-associated asthenoteratospermia. (a and b) Pedigrees of the two families with mutations in *SPAG6* or *RSPH3*. The compound heterozygous mutations in *SPAG6* (c.143_145del: p.48_49del, c.585delA: p.Lys196Serfs*6) were identified in a sporadic PCD patient and one novel homozygous nonsynonymous mutation in *RSPH3* (c.C799T: p.Arg267Cys) was identified in another patient with consanguineous parents. Sanger sequencing verified the mutations and their parental origins. (c and d) A schematic representation of SPAG6 and RSPH3 protein and the mutations identified in this study. The orange boxes indicate armadillo-type repeats domains of SPAG6 and the green box indicates the radial spoke 3 domain of RSPH3. WT, wild-type

were assessed and cultured in cleavage medium (Cook, USA) in an incubator with an environment of 37 °C, 5% O_2, 6% CO_2, and 89% N_2 until day 3 after fertilization. Then, the evaluated embryos were transferred to blastocyst medium (Cook, USA) and incubated to day 5 or day 6. According to the scoring system, all good-quality blastocysts were cryopreserved by vitrification. Two months later, 1–2 embryos were thawed and transferred for each couple. Serum β-HCG levels of the patients' partners were tested 2 weeks later, and transvaginal ultrasound was performed for the partners with elevated β-HCG levels 4 weeks after embryo transfer to assess intrauterine clinical pregnancy.

Statistical analyses

The $\chi 2$ test was employed to compare proportions between two groups, such as fertilization rate, blastocyst development rate, implantation rate, and clinical pregnancy rate. Student's *t* test was used to compare the means between two groups. *p*-values ≤ 0.05 were identified as statistically significant difference. Statistical analyses were conducted using SPSS (Windows version 16.0, IBM-SPSS, USA).

Results

Semen analysis under light microscopy

The spermatozoal parameters were summarized in Table 1. Total spermatozoa's motility ranged from 0 to 1.8%. There were no progressive motile spermatozoa in all patients and the spermatozoa were completely immotile in P1. The abnormal morphology of spermatozoa varied from 97.5 to 100%, in which flagellar abnormalities accounted for the main proportion. The five classified flagella abnormalities could account for 96–100%. Notably, short and coiled flagella represented the predominant phenotypes which were observed (Fig. 1).

Electron microscopy analysis

Over 50 cross-sectional flagellar ultrastructures were investigated by TEM for each PCD patient and normal control. The main axonemal and peri-axonemal structure defects of P1, P4, and P5 were summarized in Table S3. We found variable absence of RSs (65.4%) and the absence of CP apparatus (19.2%) in P2 and variable absence of central microtubules (88.9%) in P3 (Fig. 2). SEM showed multiple malformations of the two patients' flagella, containing short, coiled, absent, and bent. (Fig. 1).

Novel mutations in *SPAG6* and *RSPH3* were identified by WES

In consideration of the autosomal recessive inheritance pattern and rare incidence of PCD, we focused on the homozygous or potential compound heterozygous variants and filtered out the common variants according to the 1000 Genomes Project, Exome Aggregation Consortium (ExAC) Browser, and Genome Aggregation Database (gnomAD) after WES. Further, the genes with restrictive or high expression in the lung and testis were screened out and predicted by SIFT, PolyPhen-2, and MutationTaster. Intriguingly, we found that P3 carried the novel compound heterozygous mutations in *SPAG6* (Table 2). According to the previously mentioned databases, the non-frameshift mutation c.143_145del (p.48_49del) and the frameshift mutation c.585delA (p.Lys196Serfs*6) are either absent or infrequent, which is consistent with the prevalence of PCD. In addition, one novel homozygous nonsynonymous mutation c.C799T (p.Arg267Cys) in *RSPH3* was identified in P2. This infrequent mutation is predicted to be highly deleterious by all three bioinformatic tools. Sanger sequencing verified these mutations and their parental origins, and the localization of these novel mutations was ascertained (Fig. 3).

Lower expression levels of SPAG6 protein and mRNA in *SPAG6*-mutant spermatozoa

Reverse transcription q-PCR showed that *SPAG6* mRNA expression level in spermatozoa from P3 was significantly lower than that from the normal control ($p < 0.001$, Fig. 4a); however, the mRNA was not completely decayed. IF staining with anti-SPAG6 (red) and anti-acetylated tubulin (green) antibodies revealed that SPAG6 protein was located in the entire flagella of control sperm, but the protein immunostaining was extremely weak and discontinuous in P3's sperm flagella (Fig. 4c). Both results were matched together and verified the pathogenicity of this novel compound heterozygous mutations.

RSPH3 protein was absent and the mRNA was decayed in *RSPH3*-mutant spermatozoa

Compared with the control sample, the relative *RSPH3* mRNA expression level was approximately zero in P2's spermatozoa ($p < 0.001$, Fig. 4b), consistent with the absent

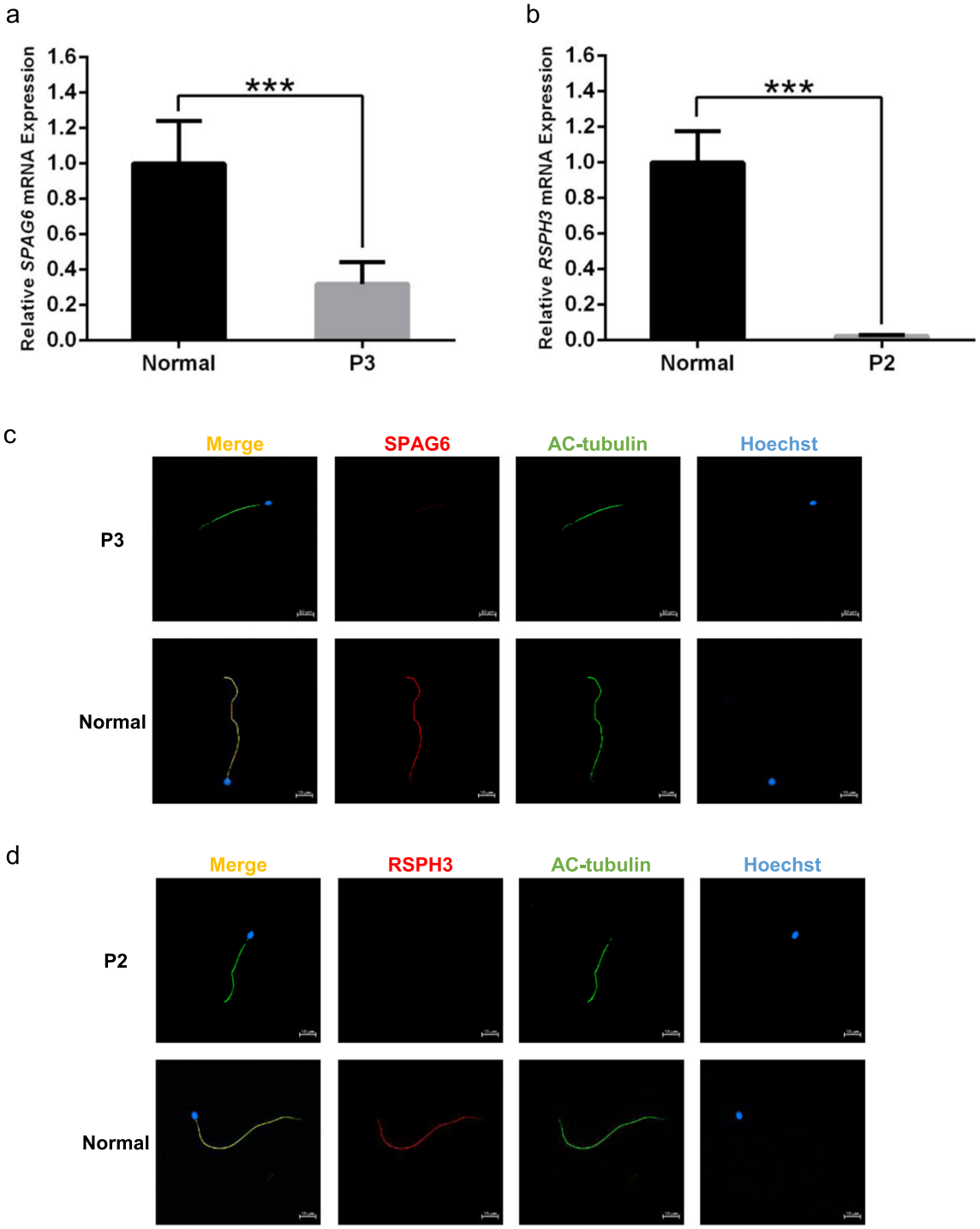

Fig. 4 mRNA expression and protein levels of *SPAG6* and *RSPH3* in the spermatozoa from P3, P2, and a healthy control man. (a) Quantitative real-time PCR (q-PCR) showed that *SPAG6* mRNA expression level in spermatozoa from P3 were significantly lower than that from the normal control $^{***}p < 0.001$ (Student's *t* test). (b) q-PCR showed that *RSPH3* mRNA expression level was approximately zero in P2's spermatozoa, significantly lower than that from the normal control $^{***}p < 0.001$ (Student's *t* test). (c) Immunofluorescence (IF) staining with anti-SPAG6 (red) and anti-acetylated tubulin (green) antibodies revealed that SPAG6 protein was located in the entire flagella of control sperm, but the protein immunostaining was extremely weak and discontinuous in P3's sperm flagella. (d) IF staining with anti-RSPH3 (red) and anti-acetylated tubulin (green) antibodies revealed that RSPH3 protein was located in the entire flagella of control sperm; however, the protein was absent from P2's sperm flagella. Scale bars represent 10 μm

RSPH3 protein in the patient's sperm flagella (Fig. 4d). These observations confirmed that this homozygous loss-of-function mutation caused the disappearance of mRNA transcribed from *RSPH3*, resulting in impaired flagella.

ICSI outcomes of PCD patients and the control groups

The ICSI outcomes of PCD, MMAF, and OAT patients are summarized in Table 3, and the results of each PCD patient are presented in Table S4. For the couples carrying mutations in *SPAG6* (P3) and *RSPH3* (P2), they both underwent one ICSI cycle and got pregnant after one frozen-thawed embryo transfer (FET) cycle. P1, P4, and P5 with no identified pathogenic gene mutation underwent four ICSI-FET cycles. P1 underwent two ICSI cycles, but pregnancy was not achieved after two cycles of FET. P4 had two gestational sacs with viable twins at the 30th day after one ICSI-FET cycle, but one of the fetuses stopped developing at the 40th day. P5 got singleton pregnancy after one ICSI-FET cycle. In total, the five PCD couples underwent six ICSI cycles and six FET cycles. Four couples got pregnant and each gave birth to a healthy child. In addition, we compared the ICSI results of the PCD patients with eight *DNAH1*-mutated MMAF patients and 215 OAT patients, respectively. There were no significant differences between PCD group and the other two groups in terms of fertilization rate, embryos development rate (eight cells and blastocyst), implantation rate, and pregnancy rate.

Discussion

Axoneme, a highly conserved microtubule-based organelle, is described as the central cytoskeletal structure shared by both motile cilium and sperm flagellum. This core component contains a central pair of microtubules (CP) and nine peripheral doublet microtubules (DMTs), circumferentially surrounding the CP apparatus. The microtubules are connected by radial spokes (RSs), outer and inner dynein arms, nexin links, and many other components [12]. To date, mutations in multiple genes, encoding axonemal proteins, have been demonstrated to cause organizational disorder of cilia and flagella, leading to PCD and male infertility [5]. Our study demonstrated that novel mutations in ciliopathy-related *SPAG6* and *RSPH3* cause infertility with severe asthenoteratospermia that can be managed by ICSI with a positive pregnancy outcome.

SPAG6, a predominantly expressed gene in the lung and testis, encodes sperm-associated antigen 6 protein (SPAG6), an axonemal protein orthologous to *C. reinhardtii* PF16 [13]. *Pf16*-mutated *C. reinhardtii* showed flagellar paralysis due to the defects of central microtubule C1, where the PF16 localized in [14]. *Spag6*-deficient mice suffered from hydrocephalus and infertility due to the impaired motility of ependymal cilia and sperm flagella [6]. These observations strongly support the importance of SPAG6 in the assembly of cilium and flagellum. Elucidation of the mechanisms is as follows: as SPAG6 is incorporated into the central apparatus, it is unambiguously important in stabilizing the axoneme; furthermore, the eight armadillo-type repeats (ARM), a key structural feature of SPAG6, are proposed to perform structural or regulatory functions by interacting with the other CP proteins [13, 15, 16]. Remarkably, SPAG6 bindings with SPAG16 and SPAG17, another component of CP, presumably regulate the function of axoneme [17, 18]. Intriguingly, for the first time,

Table 3 Clinical outcomes of ICSI among PCD, MMAF, and OAT patients

	Group A PCD	Group B MMAF (*DNAH1* mutated)	Group C OAT	p^a	p^b
No. of patients	5	8	215	/	/
Mean male age (years)	28.0 ± 3.0	30.0 ± 4.2	29.5 ± 4.0	0.374	0.396
Mean female age (years)	28.6 ± 3.4	27.9 ± 3.4	28.1 ± 3.7	0.712	0.772
No. of ICSI cycles	6	10	219	/	/
No. of oocytes injected	75	115	2692	/	/
Fertilization rate (%)	52/75 (69.3)	78/115 (67.8)	2115/2692 (78.6)	0.827	0.056
Cleavage rate (%)	50/52 (96.2)	75/78 (96.2)	2071/2115 (97.9)	> 0.999	0.700
Eight cells embryo development rate (%)	33/52 (63.5)	50/78 (64.1)	1376/2115 (65.1)	0.941	0.811
Blastocyst development rate (%)	26/52 (50.0)	41/78 (52.6)	1128/2115 (53.3)	0.774	0.634
No. of frozen-thawed embryos transfer cycles	6	13	213	/	/
Mean number of embryos transferred	1.7 ± 0.5 (10)	1.6 ± 0.5 (21)	1.6 ± 0.5 (336)	0.841	0.686
Implantation rate (%)	5/10 (50.0)	8/21 (38.1)	166/336 (49.4)	0.811	> 0.999
Clinical pregnancy rate (%) per embryos transfer cycle	4/6 (66.7)	7/13 (53.8)	122/213(57.3)	0.979	0.968
Miscarriage rate (%)	0	0	24/122 (19.7)	/	/

[a] Group A compared with group B

[b] Group A compared with group C

/, not been compared

MMAF, multiple morphological abnormalities of the sperm flagella; *OAT*, oligo-asthenospermia

the compound heterozygous mutations in *SPAG6* (c.143_145del: p.48_49del, c.585delA: p.Lys196Serfs*6) were identified in a PCD proband (P3) that resulted in infertility due to the severe asthenoteratospermia with multiple malformations of the flagella. Human SPAG6 (O75602) also comprises the highly conserved ARM domains [19]. Because these bi-allelic mutations were located at the first and fourth ARM domain, respectively, they were potentially deleterious at the protein level. Regarding the size and position of the heterozygous non-frameshift mutation c.143_145del, the variant p.48_49del might cause moderately adverse effects on SPAG6 synthesis. This inference was confirmed by q-PCR and IF analyses. Despite the mRNA expression levels of *SPAG6* in spermatozoa from P3 were significantly lower than that of the normal control, the *SPAG6* mRNA was not completely decayed, keeping with the extremely weak and discontinuous SPAG6 immunostaining in the P3's sperm flagellum. Investigation of the abnormal flagella revealed the variable absence of central microtubules which further confirmed the pathogenicity of these compound heterozygous mutations in the assembly of sperm flagella.

RSPH3, encoding a RS protein orthologous to *C. reinhardtii* RSP3, is also mainly expressed in respiratory and testicular cells [7]. RS is a T-shaped structure; its horizontal head binds to CP apparatus and the vertical stalk binds to the A-tubule of DMT. The CP-RS-DMT complex is responsible for transmitting the mechanochemical signals and regulating flagellar motility [20]. Mutations in *RSPH3* were demonstrated to cause the defects in almost all RSs and partial CP apparatus of the airway epithelial cilia in the PCD patients; however, the study did not elucidate the potentially harmful effects of those mutations in the proper building of sperm flagella in the two recruited infertile PCD men [7]. Herein, we identified a novel homozygous nonsynonymous mutation in *RSPH3* from a sterile PCD patient (P2) with severe asthenoteratospermia. RSPH3 (Q86UC2) comprises a radial spoke 3 domain (RS3D), which contains six functional domains that are well conserved in RSP3. These domains are essential for RS development by interacting with specific protein partners, such as protein kinase A, RSP11, and RSP23 [21, 22]. The novel mutation (c.C799T: p.Arg267Cys), localizing within the RS3D, is predicted to be highly deleterious by all three bioinformatic tools. Coincidentally, RT-PCR showed the mutation causing *RSPH3* mRNA decay in spermatozoa from P2 and IF verified the RSPH3 protein was obviously absent from the abnormal sperm flagella, consisting with the variable defects of RSs observed in the flagella.

Several live births following ICSI have been reported in PCD patients [23–26]. The fertilization and clinical pregnancy rates varied from 55.0 to 65.0% and from 36.4 to 50.0%, respectively [27]. For the first time, our study displayed the positive ICSI outcomes of PCD patients carrying *SPAG6* or *RSPH3* mutations, and both patients obtained their healthy offspring after one FET cycle. To prevent recessive homozygous mutations or compound heterozygous mutations inheritance to their offspring, mutation screening for *SPAG6* or *RSPH3* in their partners were performed before ICSI. Fortunately, no deleterious mutations were identified in the partners. Further, two of the other three non-genotyped PCD patients fathered a healthy boy after one cycle of ICSI-FET, respectively. As phenotypes of multiple flagellar malformations in the five infertile PCD patients were similar to those in the MMAF patients [28, 29], we compared the ICSI outcomes of the PCD patients with MMAF patients and also with the OAT patients recruited in our center. The fertilization rate, embryo development rate (eight cells and blastocyst), implantation rate, and clinical pregnancy rate in the five PCD couples were statistically comparable with the outcomes of theeight *DNAH1*-mutated MMAF couples and the 215 OAT couples in the same time period.

As previously reported, flagellar ultrastructural defects might cause the impaired centriole function [30] and elevated aneuploidy formation of spermatozoa [31, 32], resulting in abnormal embryonic development and subsequently poor ICSI outcomes. Furthermore, due to the poor sperm nuclear quality, ICSI outcomes could be significantly decreased in the presence of immotile spermatozoa [33]. In the present study, we found that morphologically normal and physiologically motile spermatozoa were available during ICSI in all PCD patients except P1; thus, the possibility that the selected spermatozoa might not carry the defects impairing the ICSI results cannot be excluded. Accordingly, the absence of motile spermatozoa as well as the unidentified ciliopathy gene might cause the poor ICSI outcomes of P1. Nevertheless, due to the small samples size, it is difficult to draw any firm conclusions concerning ICSI results in our study.

Our current investigation revealed the novel pathogenic mutations in PCD-associated *SPAG6* and *RSPH3* in male infertile patients with severe asthenoteratospermia characterized by multiple malformations of the flagella. ICSI is an optimal management with a positive pregnancy outcome. For better evaluation of the pathological effects of the PCD-associated asthenoteratospermia on the outcome of ICSI, further studies are required to elucidate the precise molecular mechanisms of the ciliopathy genes in spermatogenesis.

Funding information This study was supported by the Natural Science Foundation of Anhui Province (1908085QH313), Special Foundation for Development of Science and Technology of Anhui Province (2017070802D150 and YDZX20183400004194), National Natural Science Foundation of China (81901541 and 81971441), Non-profit Central Research Institute Fund of Chinese Academy of Medical Sciences (2019PT310002) and Shanghai Municipal Science and Technology Major Project (2017SHZDZX01).

Compliance with ethical standards

This research was approved by the ethical committee of The First Affiliated Hospital of Anhui Medical University. All participants in this study signed informed consent.

Conflict of interest The authors declare that they have no conflict of interest.

References

1. Afzelius BA. A human syndrome caused by immotile cilia. Science. 1976;193:317–9.
2. Leigh MW, Pittman JE, Carson JL, Ferkol TW, Dell SD, Davis SD, et al. Clinical and genetic aspects of primary ciliary dyskinesia/Kartagener syndrome. Genet Med. 2009;11:473–87.
3. Afzelius BA. The immotile-cilia syndrome: a microtubule-associated defect. CRC Crit Rev Biochem. 1985;19:63–87.
4. Knowles MR, Daniels LA, Davis SD, Zariwala MA, Leigh MW. Primary ciliary dyskinesia. Recent advances in diagnostics, genetics, and characterization of clinical disease. Am J Respir Crit Care Med. 2013;188:913–22.
5. Coutton C, Escoffier J, Martinez G, Arnoult C, Ray PF. Teratozoospermia: spotlight on the main genetic actors in the human. Hum Reprod Update. 2015;21:455–85.
6. Sapiro R, Kostetskii I, Olds-Clarke P, Gerton GL, Radice GL, Strauss IJ. Male infertility, impaired sperm motility, and hydrocephalus in mice deficient in sperm-associated antigen 6. Mol Cell Biol. 2002;22:6298–305.
7. Jeanson L, Copin B, Papon JF, Dastot-Le Moal F, Duquesnoy P, Montantin G, et al. RSPH3 mutations cause primary iliary dyskinesia with central-complex defects and a near absence of radial spokes. Am J Hum Genet. 2015;97:153–62.
8. He X, Li W, Wu H, Lv M, Liu W, Liu C, et al. Novel homozygous CFAP69 mutations in humans and mice cause severe asthenoteratospermia with multiple morphological abnormalities of the sperm flagella. J Med Genet. 2019;56:96–103.
9. Wu H, Li W, He X, Liu C, Fang Y, Zhu F, et al. NovelCFAP43 andCFAP44 mutations cause male infertility with multiple morphological abnormalities of the sperm flagella (MMAF). Reprod BioMed Online. 2019;38:769–78.
10. Zhu F, Liu C, Wang F, Yang X, Zhang J, Wu H, et al. Mutations in PMFBP1 cause acephalic spermatozoa syndrome. Am J Hum Genet. 2018;103:188–99.
11. de Oliveira NM, Vaca Sanchez R, Rodriguez Fiesta S, Lopez Salgado T, Rodriguez R, Bethencourt JC, et al. Pregnancy with frozen-thawed and fresh testicular biopsy after motile and immotile sperm microinjection, using the mechanical touch technique to assess viability. Hum Reprod. 2004;19:262–5.
12. Inaba K. Molecular architecture of the sperm flagella: molecules for motility and signaling. Zool Sci. 2003;20:1043–56.
13. Smith EF, Lefebvre PA. PF16 encodes a protein with armadillo repeats and localizes to a single microtubule of the central apparatus in Chlamydomonas flagella. J Cell Biol. 1996;132:359–70.
14. Adams GM, Huang B, Piperno G, Luck DJ. Central-pair microtubular complex of Chlamydomonas flagella: polypeptide composition as revealed by analysis of mutants. J Cell Biol. 1981;91:69–76.
15. Smith EF, Lefebvre PA. The role of central apparatus components in flagellar motility and microtubule assembly. Cell Motil Cytoskeleton. 1997;38:1–8.
16. Liu Y, Zhang L, Li W, Huang Q, Yuan S, Li Y, et al. The sperm associated antigen 6 interactome and its role in spermatogenesis. Reproduction. 2019;158:181–97.
17. Zhang Z, Jones BH, Tang W, Moss SB, Wei Z, Ho C, et al. Dissecting the axoneme interactome: the mammalian orthologue of Chlamydomonas PF6 interacts with sperm-associated antigen 6, the mammalian orthologue of Chlamydomonas PF16. Molecular & Cellular Proteomics. 2005;4:914–23.
18. Zhang Z, Sapiro R, Kapfhamer D, Bucan M, Bray J, Chennathukuzhi V, et al. A sperm-associated WD repeat protein orthologous to Chlamydomonas PF20 associates with Spag6, the mammalian orthologue of Chlamydomonas PF16. Mol Cell Biol. 2002;22:7993–8004.
19. Neilson LI, Schneider PA, Van Deerlin PG, Kiriakidou M, Driscoll DA, Pellegrini MC, et al. cDNA cloning and characterization of a human sperm antigen (SPAG6) with homology to the product of the Chlamydomonas PF16 locus. Genomics. 1999;60:272–80.
20. Oda T, Yanagisawa H, Yagi T, Kikkawa M. Mechanosignaling between central apparatus and radial spokes controls axonemal dynein activity. J Cell Biol. 2014;204:807–19.
21. Yang C, Yang P. The flagellar motility of Chlamydomonas pf25 mutant lacking an AKAP-binding protein is overtly sensitive to medium conditions. Mol Biol Cell. 2006;17:227–38.
22. Sivadas P, Dienes JM, St Maurice M, Meek WD, Yang P. A flagellar A-kinase anchoring protein with two amphipathic helices forms a structural scaffold in the radial spoke complex. J Cell Biol. 2012;199:639–51.
23. Kay VJ, Irvine DS. Successful in-vitro fertilization pregnancy with spermatozoa from a patient with Kartagener's syndrome: case report. Hum Reprod. 2000;15:135–8.
24. Peeraer K, Nijs M, Raick D, Ombelet W. Pregnancy after ICSI with ejaculated immotile spermatozoa from a patient with immotile cilia syndrome: a case report and review of the literature. Reprod BioMed Online. 2004;9:659–63.
25. McLachlan RI, Ishikawa T, Osianlis T, Robinson P, Merriner DJ, Healy D, et al. Normal live birth after testicular sperm extraction and intracytoplasmic sperm injection in variant primary ciliary dyskinesia with completely immotile sperm and structurally abnormal sperm tails. Fertil Steril. 2012;97:313–8.
26. Montjean D, Courageot J, Altie A, Amar-Hoffet A, Rossin B, Geoffroy-Siraudin C, et al. Normal live birth after vitrified/warmed oocytes intracytoplasmic sperm injection with immotile spermatozoa in a patient with Kartagener's syndrome. Andrologia. 2015;47:839–45.
27. Kawasaki A, Okamoto H, Wada A, Ainoya Y, Kita N, Maeyama T, et al. A case of primary ciliary dyskinesia treated with ICSI using testicular spermatozoa: case report and a review of the literature. Reprod Med Biol. 2015;14:195–200.
28. Ben Khelifa M, Coutton C, Zouari R, Karaouzene T, Rendu J, Bidart M, et al. Mutations in DNAH1, which encodes an inner arm heavy chain dynein, lead to male infertility from multiple morphological abnormalities of the sperm flagella. Am J Hum Genet. 2014;94:95–104.
29. Tang S, Wang X, Li W, Yang X, Li Z, Liu W, et al. Biallelic mutations in CFAP43 and CFAP44 cause male infertility with multiple morphological abnormalities of the sperm flagella. Am J Hum Genet. 2017;100:854–64.
30. Schatten H, Sun QY. The role of centrosomes in mammalian fertilization and its significance for ICSI. Mol Hum Reprod. 2009;15:531–8.

31. Rives N, Mousset-Simeon N, Mazurier S, Mace B. Primary flagellar abnormality is associated with an increased rate of spermatozoa aneuploidy. J Androl. 2005;26:61–9.
32. Ghedir H, Mehri A, Mehdi M, Brahem S, Saad A, Ibala-Romdhane S. Meiotic segregation and sperm DNA fragmentation in Tunisian men with dysplasia of the fibrous sheath (DFS) associated with head abnormalities. J Assist Reprod Genet. 2014;31:1167–74.
33. Liu J, Nagy Z, Joris H, Tournaye H, Smitz J, Camus M, et al. Analysis of 76 total fertilization failure cycles out of 2732 intracytoplasmic sperm injection cycles. Hum Reprod. 1995;10:2630–6.